



Third-order optical nonlinearity and power limiting characteristics of acid green 3 dye

S HEMALATHA and T GEETHAKRISHNAN*

Department of Physics, University College of Engineering Villupuram (A Constituent College of Anna University: Chennai), Villupuram 605103, India

*Author for correspondence (tgeethakrishnan@hotmail.com)

MS received 14 February 2022; accepted 5 July 2022

Abstract. Third-order optical nonlinearity and optical limiting (OL) characteristics of an organic dye acid green 3 (AG 3) dye in water has been studied using a 635 nm diode laser of 5 mW power. The UV–visible absorption studies were carried out to understand the linear optical properties of acid green 3 dye. The recorded Fourier transform infrared spectra of acid green 3 dye reveals that the π -electrons are delocalized through intermolecular charge transfer (ICT) within the *N*-ethyl–sodium sulphite bonds, which lead to measurable polarization across the push–pull molecules. The structural properties and crystalline size of the acid green 3 dye were examined by X-ray diffraction spectra. The third-order nonlinear optical (NLO) parameters such as nonlinear absorption coefficient (β) and nonlinear refractive index (n_2) were determined by performing the open aperture Z-scan and closed aperture Z-scan experiments, respectively. The reverse saturable absorption and self-defocusing type optical nonlinearity were observed for acid green 3 dye. The experiments were also performed to understand the OL characteristics of acid green 3 dye and obtained a low limiting threshold of $1.23 \times 10^2 \text{ W cm}^{-2}$. The results of present experimental study reveal that acid green 3 dye possess good NLO properties and this dye system may be suitable for applications in low power NLO and photonic devices.

Keywords. Acid green 3 dye; FTIR; XRD; Z-scan; optical power limiting.

1. Introduction

Materials with larger optical nonlinearities have shown vast interest in the field of nonlinear optics (NLO) due to their widespread applications in phase–conjugation, optical computing, optical limiting (OL), optical image processing and many other usages in optoelectronics [1]. During laser beam propagation, nonlinear media with intensity-dependent refractive index and absorption coefficient exhibit a variety of fascinating phenomena. Organic NLO materials with large optical nonlinearities are particularly appealing in this context due to their fast response time, broadband spectral response, low-cost and easier preparations [2]. A wide range of organic NLO materials such as metal–liquid crystal complexes [3], gold nanoparticles [4], chemical compounds [5] and organic dyes [6,7] exhibit excellent third-order optical nonlinearity. The special features of organic dye-compatible diode lasers have helped biomolecular science and pharmaceutical applications throughout the last few decades [8–10]. Organic dye molecules possess delocalized π -electrons, which show an excellent molecular polarizability and rapid redistribution of charges in high electric field strength [11–13]. Intramolecular transfer of charges between the strong electron donor and acceptor groups aids in enhancing the

molecular hyperpolarizabilities, which stabilizes the system and improves the NLO activities in a conjugated molecular system. These conjugated structure-based compounds facilitate electron transfer between donor and acceptor groups, resulting in efficient π -electron delocalization and therefore increased nonlinearity. Many researchers have already reported the third-order NLO behaviour of various organic dyes, utilizing the high power lasers available, namely triphenylmethane, red biebrich scarlet (BS) dye, anthraquinone and many other natural dyes [14–19].

The present acid green 3 (AG 3) dye under investigation belongs to the class of triarylmethane (TAM). TAM dyes are synthetic organic compounds with a central carbon atom linked to three aromatic rings, the colour and properties depending on the number and nature of auxo chromic groups. They are the most widely used of the arylmethane dyes and are known for their bright colours, making them excellent staining agents. These dyes consist of delocalized π -electrons in both their nucleus and substituent bodies [20]. AG 3 dye exhibits π -conjugated planar structure that includes donor and acceptor groups, which originate the NLO behaviour and makes them suitable for many NLO devices. Optical limiters (OL) use nonlinear optical (NLO) materials to shield human eyes, electronic devices, and solid-state optical sensors from dangerous laser beams.

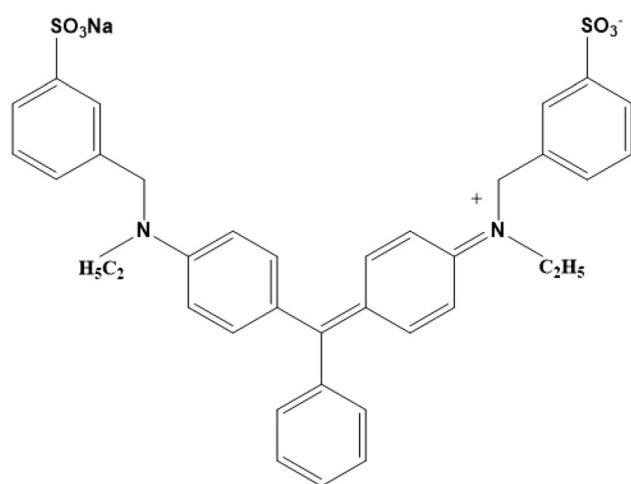
Optical limiters have a linear light transmission for the lower input intensities, whereas, at higher light intensities, they are designed to have a stable or a saturable light transmission. In OL studies, the NLO properties of organic dye molecules have attracted a great deal of attention because of their significant characteristics of higher damage threshold, linear beam transmittance at low input power and a minimum threshold [21,22].

This paper reports the nonlinear absorption (NLA) coefficient β , refractive index n_2 , susceptibility $\chi^{(3)}$ and OL characteristics of acid green 3 (AG 3) using Z-scan experiments, which utilizes a continuous wave diode laser (635 nm, 5 mW). The closed aperture Z-scan, open aperture Z-scan and OL studies were carried out for aqueous solutions of AG 3 dye at an input intensity of $1.135 \times 10^3 \text{ W cm}^{-2}$.

2. Experimental

2.1 Materials

From Sigma Aldrich, India Ltd, acid green 3 dye (AG 3) was procured and used as received for the present study. AG 3 dye powder appears as dull green shade and it is highly soluble in water. The chemical formula and the molecular structure of AG 3 dye are shown in figure 1. A spectrophotometer (Model No: Perkin Elmer Lambda 35) was used to record the UV–visible absorption spectrum of AG 3 dye. Fourier transform infrared (FTIR) spectrum of the AG 3 dye was recorded using a Perkin–Elmer infrared spectrometer with an attenuated total reflectance (ATR) in the wavenumber range of $4000\text{--}400 \text{ cm}^{-1}$ at transmittance mode. The X-ray diffraction (XRD) measurements were carried out using the diffractometer (PANalytical XRAY)



Molecular formula: $\text{C}_{37}\text{H}_{35}\text{N}_2\text{NaO}_6\text{S}_2$

Figure 1. Chemical structure and molecular formula of AG 3 dye.

with $\text{CuK}\alpha$ wavelength of 1.5406 \AA . The 2θ scanning range was fixed as $10^\circ\text{--}90^\circ$ with a stepping interval of 0.01° .

3. Z-scan measurements

The single beam Z-scan technique developed by Sheik-Bahae *et al* [23] is a standard tool to measure the sign and magnitude of nonlinear index of refraction (n_2), NLA coefficient (β) and susceptibility $\chi^{(3)}$ of NLO materials. The Z-scan experimental set-up which has been used to study the aqueous solutions of AG 3 dye is shown in figure 2. A semiconductor diode laser of 635 nm wavelength with a total power of 5 mW was used to perform the Z-scan experiments. The laser beam was focused by a convex lens (focal length: 5 cm), which produces a spot size ω_0 and the Rayleigh length Z_R of $16.75 \mu\text{m}$ and 1.38 mm , respectively, in the sample. The aqueous solution of AG 3 dye sample was kept in a 1-mm thickness cuvette and the same is mounted on a translated stage, moved along the z-direction and simultaneously the intensity of the light transmitted is measured using an optical power meter. As the Rayleigh length Z_R is greater than that of the sample length L , the thin sample approximation has been assumed in the present study.

4. Results and discussions

4.1 UV–visible spectroscopy studies

The recorded optical absorption spectra of aqueous solutions of AG 3 dye samples with concentrations of 0.01, 0.02 and 0.03 mM are shown in figure 3. This spectrum exhibits a strong absorbance around 316 nm in the ultraviolet region, strong and peak absorbance, respectively, at 430 and 620 nm in the visible region. The UV absorbance observed around 316 nm is attributed to $\pi\text{--}\pi^*$ transitions and this may be due to π -conjugated electrons present in the aromatic rings, while the absorbance observed at around 430 and 620 nm is assigned to $n\text{--}\pi^*$ transitions. The absorption peak is observed mainly due to $n\text{--}\pi^*$, $\pi\text{--}\pi^*$ transition and due to the excitation of C=O, C=C group of the acid green 3 dye molecule. The UV–visible absorption bands are ascribed to the electronic charge transfer between the groups of electron–donors and electron–acceptors [24]. In AG 3 dye, the presence of an N-ethyl group in the substituent position acts as groups of electron donor that increases the conjugation length by giving electrons to the molecule's backbone. The electrons from the benzene ring are accepted by the sodium sulphite ions, which operate as the groups of electron withdrawal. As a result, the structure of donor– π -acceptor (D– π -A) is present in the AG 3 dye. Hence, the observed nonlinearity is caused by electrons pushing and pulling in the molecular system, resulting in high third-order nonlinearity. It is observed from figure 3 that the absorbance of the AG 3 dye was found to increase when

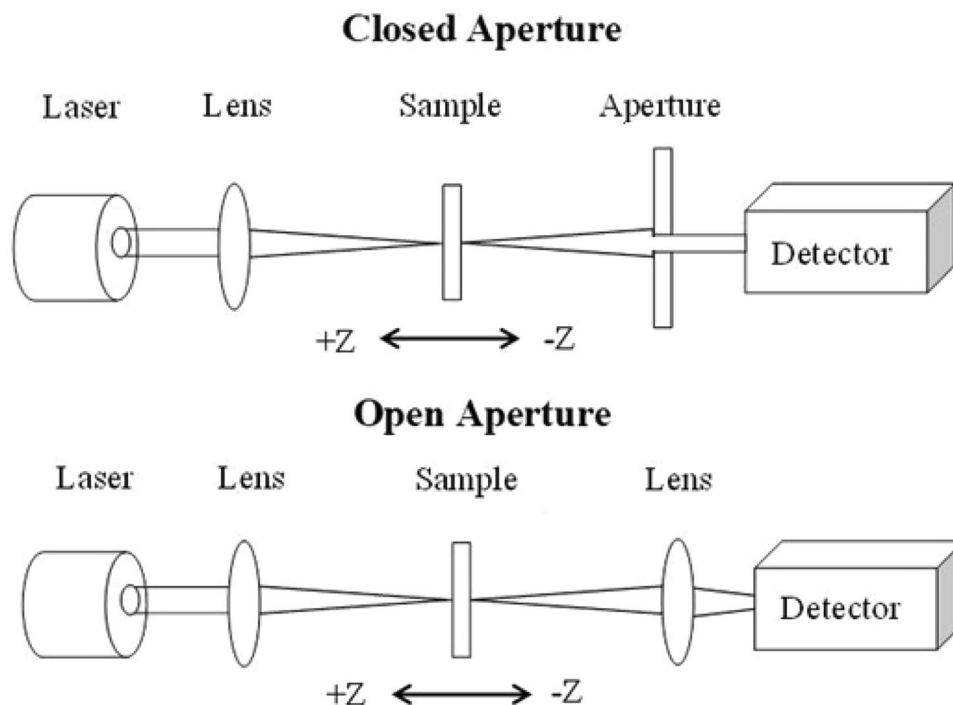


Figure 2. Experimental set-up of Z-scan technique.

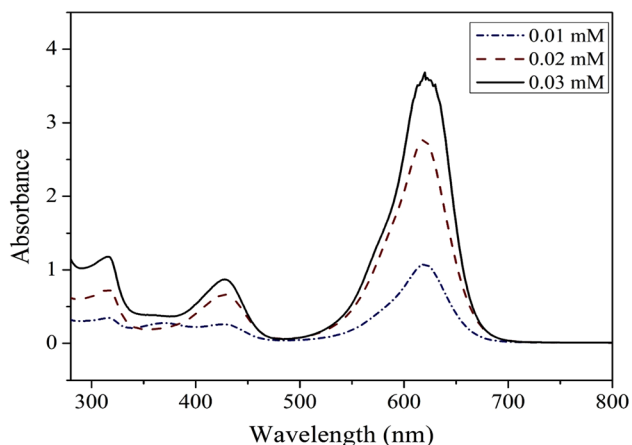


Figure 3. UV-visible absorption spectra of aqueous solutions of AG 3 dye.

the concentration of the dye molecules increases and this may be due to the fact that greater the number of molecules participated, larger the linear absorption coefficient. The measured linear absorption coefficients of aqueous solutions of AG 3 dye with concentrations of 0.01, 0.02 and 0.03 mM are presented in table 1.

5. FTIR analysis

The recorded FTIR spectrum of the AG 3 dye powder is shown in figure 4, a strong correlation between the bands is observed in the present case and the peaks are assigned

Table 1. Linear absorption coefficients of aqueous solutions of AG 3 dye.

Concentration (mM)	Linear absorption coefficient (cm^{-1})
0.01	0.72
0.02	1.39
0.03	2.35

based on the literature [25,26]. The hydrogen bond O–H stretching vibrations are responsible for strong broadband peaked at 3440 cm^{-1} . The peak observed at 2940 cm^{-1} can be assigned to the asymmetric and symmetric C–H stretching of the alkyl groups, while the strong band observed at 1739 cm^{-1} are attributed to the C=O stretching vibration of the aldehyde groups. The medium band peak observed at 1644 cm^{-1} corresponds to C=C stretching vibrations of alkenes, which shows stronger connection with NLO properties due to its conjugate moiety with π -electron chain. The dipole moment and polarizability of the dye molecules gets improved because of the ICT method through a single-double bond conjugated path between groups of electron donor to the acceptor. The modes of C=C stretching provides the occurrence of ICT in the π -conjugated system and thus, C=C stretching modes contribute to the formation of several medium and strong bands in the spectrum of AG 3 dye molecules at 1558 , 1518 and 1476 cm^{-1} . This indicates that the molecules of AG 3 dye are extremely polarized, which in turn improves the NLO properties. The peak observed at 1344 cm^{-1} appears

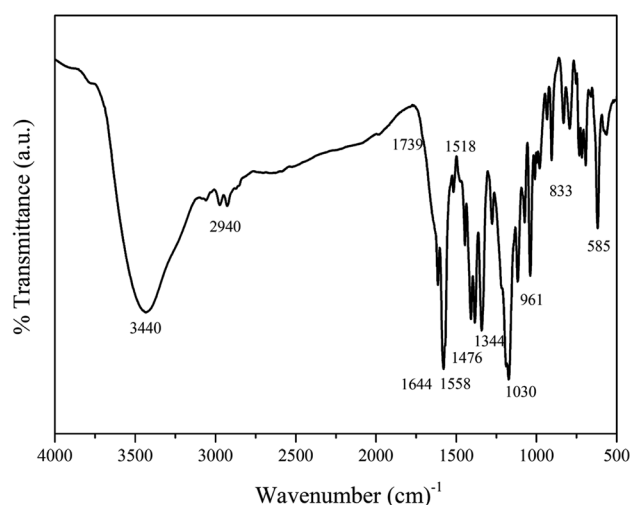


Figure 4. Recorded FTIR spectrum of AG 3 dye.

as medium band, which corresponds to the N–O asymmetric stretching vibrations of nitro compounds. The vibrational band which is observed at 1086 cm^{-1} may be due to the stretching of the acetyl groups that exists in the AG 3 dye molecule. The observed absorption peaks at 961 and 833 cm^{-1} are respectively attributed to the bending of alkene C=C and vibrations of skeletal bands. The recorded FTIR wavenumbers of acid green 3 dye samples are comparable with that of similar molecules, which have been reported in recent literatures [27–33], and the results are presented in table 2.

6. XRD analysis

The measured XRD patterns of AG 3 dye powder is shown in figure 5. The XRD pattern reveals many sharp and intense reflection peaks and this indicates that the dye molecules are highly crystalline in nature [34,35]. The XRD pattern of AG 3 dye powder with diffraction peaks which correspond to (hkl) planes of (111), (200), (220), (222), (400), (420) and (422), were observed at 27.29° , 31.68° , 45.39° , 56.44° , 66.25° , 75.22° and 83.88° , respectively. The

sharpness of the peaks reveals that AG 3 dye powder has high quality of the crystalline perfection. The crystalline size of AG 3 dye in powder form is calculated using Debye–Scherrer formula:

$$D = \frac{0.9\lambda}{\beta \cos\theta} \text{ nm}, \quad (1)$$

where D is the crystalline size, λ the wavelength of X-ray radiation, θ is Bragg diffraction angle and β the full width at half-maximum intensity, and the crystalline size of the AG 3 dye powder is calculated to be 20.58 nm.

7. Nonlinear absorption and nonlinear refraction

Third-order NLA coefficients (β) and nonlinear refractive indices (n_2) of aqueous solutions of AG 3 dye were calculated correspondingly from the Z-scan measurements of OA and CA methods. Figure 6 shows the traces obtained for open aperture Z-scan measurements for aqueous solutions of AG 3 dye with the concentrations of 0.01, 0.02 and 0.03 mM (incident intensity $I_0 = 1.135 \times 10^3\text{ W cm}^{-2}$). The transmitted laser beam seems to be at low intensity as the sample is located far from the focus, and the corresponding normalized transmittance is approximately 1; the beam transmission increases monotonically as the sample approaches the focal point and this exhibits the characteristics of saturable absorption (SA). The occurrence of normalized transmittance curve near the focal point with a fine peak or a deep valley corresponds to the indication of saturable absorption (SA) or reverse saturable absorption (RSA) behaviour of the sample under study [36,37]. In the present case, the sample AG 3 dye exhibits the reduction in transmittance curve with increased intensity forming a definite deep valley at the focus for all the concentrations of AG 3 dye aqueous solutions studied, which stipulate the RSA behaviour or positive NLA. Several NLO phenomena, such as two-photon absorption, excited state absorption (ESA), free carrier absorption and RSA, can generate NLA in materials. Figure 7 shows the five-level model energy diagram, which can be used to validate the NLA behaviour for the present AG 3 dye molecules. S_0 , S_1 and S_2 are respectively the singlet ground, singlet first excited state and

Table 2. Comparison of FTIR wavenumbers of AG 3 dye with recent reports.

	Peak positions (cm^{-1})	Peak assignments	References
AG 3 dye	Literature reports		
3440	3441 (Carmoisine dye)	O–H stretching	[27]
2940	2963 (Styrylquinolinium dye)	asymmetric C–H group	[28]
1739	1731 (Zinc Phthalocyanine – PVA)	C=O stretching aldehyde	[29]
1644	1640 (Bromophenol dye – silica)	C=C stretching vibration of alkene	[30]
1476	1440 (Methylsilicon phthalocyanine – PVA)	Bending and wagging of CH_2 vibrations	[31]
1080	1088 (Light green dye – PVA)	C–O stretching of acetyl groups	[32]
961	922 (Xylenol orange dye – ADP)	Bending of alkene C=C	[33]

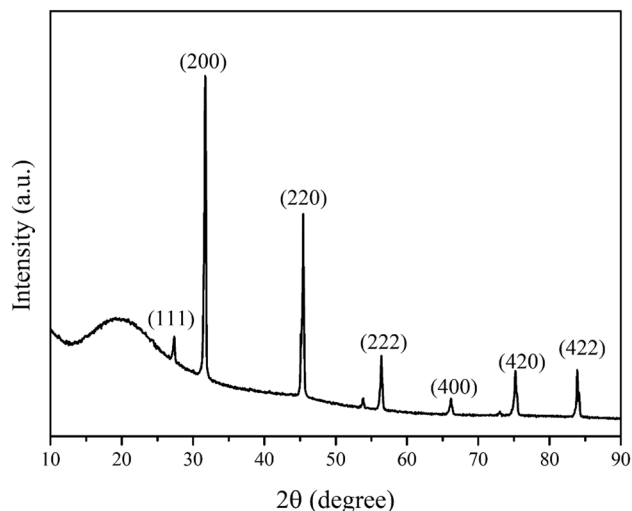


Figure 5. Recorded XRD pattern of AG 3 dye.

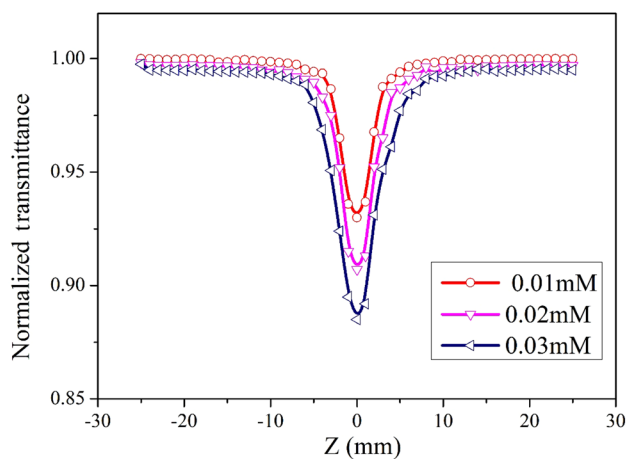


Figure 6. Open aperture Z-scan curve of aqueous solutions of AG 3 dye.

the singlet next higher excited states. Similarly, T_1 and T_2 are triplet first and triplet higher excited states, respectively. Two-photon absorption is the instantaneous absorption of two photons with either the same or distinct energy values from the ground level state to the excited level state (S_0-S_1). This transition energy process can be carried out, which is equivalent to the sum of absorption of two photons. ESA is the NLA process in which the molecules are excited from the first level excited state to the higher excited state (S_1-S_2) or (T_1-T_2). To achieve this, the population of the first level excited state (S_1 and/or T_1) must be large enough to increase the possibility of photon absorption from the state [38]. When electrons from the first level singlet excited state S_1 are shifted to the first level triplet excited state T_1 via intersystem crossing, transitions to higher level excited state T_2 are possible, which potentially improves the ESA or RSA. RSA is the NLA process in which the excited state absorption cross-section is greater than that of the ground

state absorption. The stimulated thermal effects caused by CW laser excitation rise ESA, implying that ESA-assisted RSA is the major nonlinear process causing the observed nonlinearity in AG 3 dye molecules. The transmittance from open aperture Z-scan method is represented by

$$T(z, s = 1) = \sum_{m=0}^{\infty} \frac{[-q_0(z)]^m}{[m + 1]^{\frac{3}{2}}}, \text{ for } |q_0(0)| < 1 \quad (2)$$

where

$$q_0(z) = \frac{\beta_{\text{eff}} I_0 L_{\text{eff}}}{1 + \frac{z^2}{Z_0^2}} \quad (3)$$

Here β_{eff} is the NLA coefficient obtained from open aperture Z-scan data, which is given by $\beta_{\text{eff}} = \frac{2\sqrt{2}\Delta T}{I_0 L_{\text{eff}}}$, L_{eff} is the effective thickness of the sample, which is defined as $L_{\text{eff}} = \frac{(1-e^{-\alpha L})}{\alpha}$, I_0 is the focal point beam intensity of the laser, α is the linear coefficient of absorption, Z_0 is the diffraction length and L is the sample thickness.

The CA experiment of Z-scan was carried out to determine the coefficient of nonlinear refractive index n_2 of the AG 3 dye. In this case, an aperture (linear aperture transmittance of $S = 0.4$) is placed in front of the detector and the beam transmittance is collected in the far field, the measurements are repeated for AG 3 dye aqueous solution of various concentrations chosen (0.01, 0.02 and 0.03 mM). For the present CA measurements, the normalized beam transmittance of a maximum (peak) followed by a minimum (valley) has been observed for all the samples under study. The peak-valley shape implies a negative nonlinear refraction (NLR), inferring self-defocusing behaviour. NLR can have a physical origin that is electronic, molecular, electrostrictive or thermal [39–41]. Under CW laser beam irradiation of 635 nm wavelength, the optical nonlinearity of AG 3 dye is expected to be thermal origin. This may possibly be due to the localized absorption of a strongly focused laser beam, transmitting through an absorbing media of AG 3 dye, induces a thermal and density variations that could modify the index of refraction profile and simultaneously act as a thermal optical lens. For a thermal nonlinearity, the separation of peak-valley for the Z-scan measurements (CA method) along the beam direction is given by

$$\Delta Z_{p-v} = 1.7 Z_R \quad (4)$$

From figure 8, ΔZ_{p-v} is greater than 1.7 times Z_R , which is the confirmation of thermal nonlinearity.

The Z-scan transmittance of CA method and the nonlinear index of refraction n_2 for aqueous solutions of AG 3 dye are calculated respectively from the following relations,

$$T(z) = 1 - \Delta\phi_0 \frac{4X}{(X^2 + 1)(X^2 + 9)} \quad (5)$$

$$n_2 = \frac{\Delta\phi_0 \lambda}{2\pi I_0 L_{\text{eff}}} \left(\frac{\text{cm}^2}{\text{W}} \right) \quad (6)$$

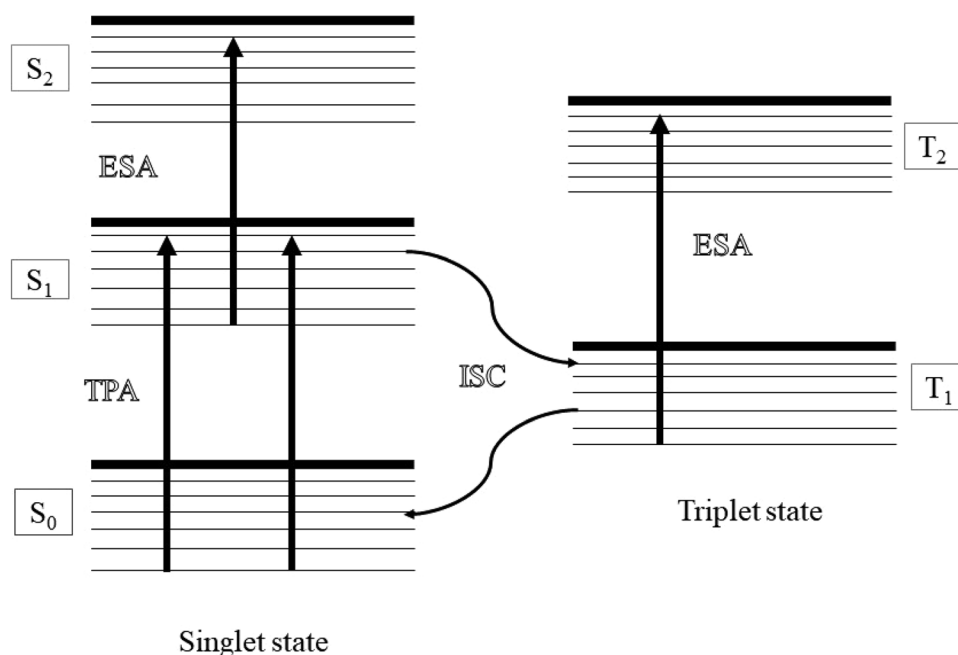


Figure 7. Energy level model for AG 3 dye molecule.

Here $X = Z/Z_0$, $\Delta\phi_0$, λ and I_0 be the on-axis phase shift, wavelength of the laser beam and incident input intensity of the laser beam.

Generally, CA transmittance is affected by NLA and NLR, and thus for determining n_2 and to separate the effect of NLR from NLA, an approximate method, i.e., dividing the CA transmittance by the corresponding OA transmittance is applied to obtain pure n_2 . Figure 8 shows the pure NLR traces obtained for aqueous solutions of AG 3 dye with dye concentrations of 0.01, 0.02 and 0.03 mM. The real and imaginary parts of the third-order NLO susceptibility $\chi^{(3)}$ is given by,

$$\text{Re} [\chi^{(3)}] (\text{esu}) = \frac{\varepsilon_0 c^2 n_0^2}{\pi} n_2 \times 10^{-4} \left(\frac{\text{cm}^2}{\text{W}} \right) \quad (7)$$

$$\text{Im} [\chi^{(3)}] (\text{esu}) = \frac{\varepsilon_0 c^2 n_0^2 \lambda}{4\pi^2} \beta \times 10^{-2} \left(\frac{\text{cm}}{\text{W}} \right) \quad (8)$$

where ε_0 = free space permittivity, c = velocity of light. The susceptibility $\chi^{(3)}$ of AG 3 dye in water is calculated by the relation,

$$\chi^{(3)} = \left[\left(\text{Re}(\chi^{(3)}) \right)^2 + \left(\text{Im}(\chi^{(3)}) \right)^2 \right]^{1/2} (\text{esu}) \quad (9)$$

The measured NLO parameters such as n_2 , β and $\chi^{(3)}$ values of AG 3 dye in water are given in table 3. It is observed that the value of third-order NLO parameters of AG 3 dye has been increased with an increase in dye concentration. This may be due to the fact that more number of AG 3 dye molecules interact with the 635 nm laser beam, which could result in increased dipole moment of the AG 3 dye molecules and hence presents the better optical nonlinearities. The third-order NLO parameters of some similar organic molecules which have been reported in the recent literature [16,18,28,42–46] under CW laser excitation are analysed, their results are comparable with our present experimental results, and the data are listed in table 4. From this, it is worth noting that the diode laser utilized for the present case is of only 5 mW powers, such category of lasers are easy available in the market and owing to this we believe that the AG 3 dye system investigated in the present work may be suitable better for the NLO applications in the low power regime.

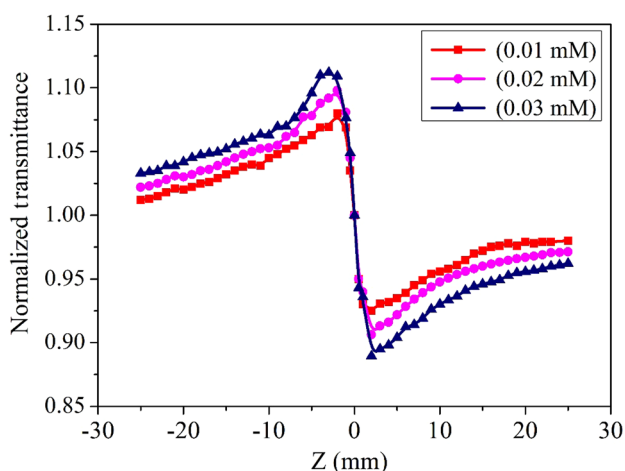


Figure 8. Pure nonlinear refraction Z-scan curves of aqueous solutions of AG 3 dye.

Table 3. NLO parameters obtained for aqueous solutions of AG 3 dye at 635 nm (incident intensity $I_0 = 1.135 \times 10^3 \text{ W cm}^{-2}$).

Dye concentration (mM)	ΔT_{P-V}	$n_2 \times 10^{-10} (\text{cm}^2 \text{ W}^{-1})$	$\beta \times 10^{-3} (\text{cm W}^{-1})$	$ \chi^{(3)} \times 10^{-7} (\text{esu})$
0.01	0.15	3.87	1.81	4.11
0.02	0.185	4.94	2.48	5.63
0.03	0.217	6.07	3.22	7.30

Table 4. Literature reports on NLO parameters under low power CW laser.

Materials	Wavelength (nm)	$n_2 (\text{cm}^2 \text{ W}^{-1})$	$\beta (\text{cm W}^{-1})$	$ \chi^{(3)} (\text{esu})$	References
Brilliant Green dye	632.8	—	1.30×10^{-3}	3.069×10^{-7}	[16]
Laccic acid dye	532	6.29×10^{-10}	0.58×10^{-9}	—	[18]
Carmoisine dye	532	-4.723×10^{-8}	-0.4898×10^{-4}	0.2337×10^{-5}	[27]
Acid blue 40 dye	632.8	-0.68×10^{-7}	-0.17×10^{-2}	0.25×10^{-6}	[42]
Amido Black 10 B dye – PVA	632.8	-1.66×10^{-7}	-0.0016	2.06×10^{-6}	[43]
1,4-Diamino 9,10- anthraquinone dye	532	1.0361×10^{-6}	2.1×10^{-4}	4.9007×10^{-5}	[44]
Toluidine Blue O dye – PVA	632.8	-0.120×10^{-6}	-2.77×10^{-6}	7.66×10^{-5}	[45]
Reactive blue 19 dye	632.8	-0.64×10^{-7}	2.32×10^{-3}	2.32×10^{-7}	[46]

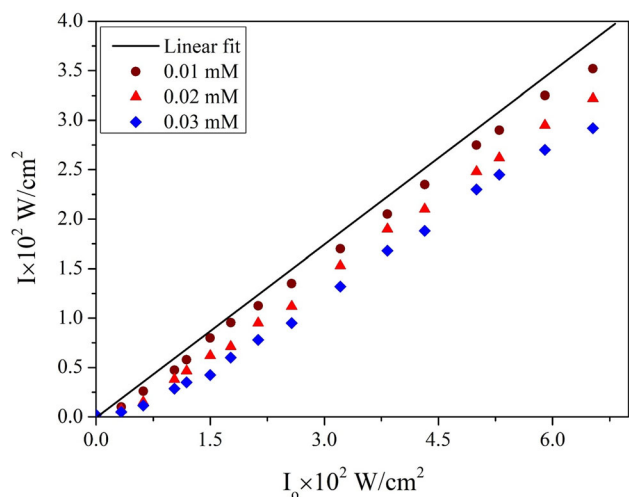


Figure 9. Optical limiting characteristics of aqueous solutions of AG 3 dye.

Table 5. Optical limiting parameters obtained for aqueous solutions of AG 3 dye at 635 nm (incident intensity $I_0 = 1.135 \times 10^3 \text{ W cm}^{-2}$).

Dye concentration (mM)	Optical limiting threshold ($I \times 10^2 \text{ W cm}^{-2}$)
0.01	1.80
0.02	1.52
0.03	1.23

8. Optical limiting

Optical limiting (OL) behaviour of the sample were also carried out, the Z-scan of OA arrangement was used in which the sample is kept precisely at the focal point. A neutral density filter is utilized to differ the input intensity of laser beam and subsequently transmitted intensity was determined by a digital power meter. Figure 9 shows the OL behaviour of AG 3 dye in water of different dye concentrations of 0.01, 0.02 and 0.03 mM. A linear relationship was observed between the input beam and output beam intensity at low input intensities which obeys Beer’s law. During the process of OL, the beam transmittance becomes nonlinear as the input intensity of the beam is increased [47,48]. The measured OL threshold parameters for aqueous solutions of AG 3 dye samples of various dye concentrations are presented in table 5. It is obvious that the limiting threshold value gets decreased as the concentration of AG 3 dye molecules gets increased in the sample, and this may be due to the fact that as the number of dye molecules gets increased which in turn increases the NLO and hence the OL efficiency.

9. Conclusion

Nonlinear optical (NLO) and OL properties of AG 3 dye in water was studied experimentally using a 5 mW diode laser working at 635 nm. The UV–visible spectra show the absorption bands around 316, 430 and 620 nm. The FTIR

analysis confirms the occurrence of intermolecular charge transfer in AG 3 dye molecules. The XRD result shows that AG 3 dye exhibits good crystalline nature, and the measured crystalline size is found to be 20.58 nm. The closed aperture Z-scan and open aperture Z-scan measurements respectively confirm the negative nonlinear index of refraction of thermal origin and RSA behaviour of AG 3 dye molecules. The measured NLO susceptibility $\chi^{(3)}$ of AG 3 dye is found to be of the order of 10^{-7} esu. Further, AG 3 dye samples exhibits good OL response with limiting threshold of 1.23×10^2 W cm^{-2} at 635 nm wavelength. The results of this work endorse that AG 3 dye possess good optical qualities of a NLO material and may have potential application in suitable NLO devices.

References

- [1] Agarwal G P and Boyd R W 1992 *Contemporary nonlinear optics quantum electronics-principles and application series* (New York)
- [2] Manikandan M, Rajesh P, Ramasamy P and Kamlesh Kumar M 2020 *Appl. Phys. A* **126** 1
- [3] Gomez S L, Cuppo F L S and Figueiredo Neto A M 2003 *Braz. J. Phys.* **33** 813
- [4] Castro H P S, Wender H and Alencar M A R C 2013 *J. Appl. Phys.* **114** 1
- [5] He G S, Xu G S, Prasad P N, Reinhardt B A, Bhatt J C and Dillard A G 1995 *Opt. Lett.* **20** 435
- [6] Geethakrishnan T and Palanisamy P K 2007 *Opt. Commun.* **270** 424
- [7] Jamshidi Ghaleha K, Salmania S and Ara M H M 2007 *Opt. Commun.* **271** 551
- [8] Kramer M A, Tompkin W R and Boyd R W 1986 *Phys. Rev. A* **34** 2026
- [9] Bredas J L, Adant C, Tackx P and Persoons A 1994 *Chem. Rev.* **94** 243
- [10] Nalwa H S 1993 *Adv. Mater.* **5** 341
- [11] Anandana S, Manoharana S, Siji Narendranb N K, Sabari Girisunb T C and Asiri A M 2018 *Opt. Mater.* **85** 18
- [12] Henari F Z 2001 *J. Opt. A: Pure Appl. Opt.* **3** 188
- [13] Geethakrishnan T and Palanisamy P K 2006 *Pramana – J. Phys.* **66** 473
- [14] Nasser F, Rokhsat E and Dorrnian D 2016 *Optik (Stuttg)* **127** 6813
- [15] Sreenath M C, Hubert Joe I and Rastogi V K 2018 *Opt. Laser Technol.* **108** 218
- [16] Choubey R K, Medhekar S, Kumar R, Mukherjee S and Sunil K 2014 *J. Mater. Sci. Mater. Electron.* **25** 1410
- [17] Ali Q M and Palanisamy P K 2005 *Optik* **116** 515
- [18] Zongo S, Sanusi K, Britton J, Mthunzi P, Nyokong T, Maaza M *et al* 2015 *Opt. Mater.* **46** 270
- [19] Thankappan A, Thomas S and Nampoore V P N 2012 *J. Appl. Phys.* **112** 1
- [20] Ley C, Brendle J, Walter A, Jacques P, Ibrahima A and Allonasa X 2015 *Phys. Chem. Chem. Phys.* **17** 16677
- [21] Rekha R K and Ramalingam A 2009 *Am. J. Appl. Sci.* **2** 285
- [22] Harilal S, Bindhu C V, Nampoore V P N and Vallabhan C P G 1999 *J. Appl. Phys.* **86** 1388
- [23] Sheik-Bahae M, Said A A, Wei T, Hagan D J and Van Stryland E W 1990 *IEEE J. Quant. Elect.* **26** 760
- [24] MigalskaZalas A, Korchi K E L and Chtouki 2018 *Opt. Quantum Electron.* **50** 1
- [25] Sajana D, Ravindra H J, Misrac N and Hubert Joe I 2010 *Vib. Spectrosc.* **54** 72
- [26] Goel N, Sinha N and Kumar B 2013 *Opt. Mater.* **35** 479
- [27] Abdullaha M, Bakhtiarb H, Krishnan G, Aziz M S A, Daniald W H and Islamb S 2019 *Opt. Laser Technol.* **108** 218
- [28] El Ouazzani H, Dabos-Seignon S, Gindre D, Iliopoulos K, Todorova M, Bakalska R *et al* 2012 *J. Phys. Chem. C* **116** 7144
- [29] Viswanath V, Subodh G and Muneera C I 2020 *Opt. Laser Technol.* **127** 106168
- [30] Islam S and Abdullah M 2020 *Opt. Mater.* **106** 110034
- [31] Saleem I Qashou, El-Zaidia E F M, Darwish A A A and Hanafy T A 2019 *Phys. B: Condens. Matter.* **571** 93
- [32] Sreeja S, Sreedhanya S, Smijesh N, Reji Philip and Muneera C I 2013 *J. Mater. Chem. C* 1
- [33] Goel S, Sinha N, Yadav H, Abhilash Joseph J, Hussain A and Kumar B 2017 *Arab. J. Chem.* **3006** 1
- [34] Das R and Kumar R 2012 *Mater. Res. Bull.* **47** 239
- [35] Durgababu G, Nagaraju G J and Bhagavannarayana G 2021 *J. Mater. Sci. Mater. Electron.* **32** 2564
- [36] Geethakrishnan T, Sakthivel P and Palanisamy P K P 2015 *Opt. Commun.* **375** 218
- [37] Madhana Sundari R and Palanisamy P K 2006 *Appl. Surf. Sci.* **252** 2281
- [38] Santhi A, Vinu Nambodiri V, Radhakrishnan P and Nampoore V P N 2006 *J. Appl. Phys.* **100** 053104
- [39] Geethakrishnan T and Palanisamy P K 2005 *Curr. Sci.* **89** 1894
- [40] Zidan M D, Ajji Z, Allaf A W and Allahham A 2011 *Opt. Laser Technol.* **43** 1347
- [41] Geethakrishnan T and Palanisamy P K 2006 *Optik* **117** 282
- [42] Pramodini S, Poornesh P and Nagaraja K K 2013 *Curr. Appl. Phys.* **13** 1175
- [43] Sreekumar G, Louie Frobel P G, Muneera C I, Sathiyamoorthy K, Vijayan C and Mukherjee C 2009 *J. Opt. A: Pure Appl. Opt.* **11** 125204
- [44] Zafar S, Khan Z H and Khan M 2013 *Spectrochim. Acta Part A Mol. Biomol. Spectrosc.* **114** 164
- [45] Viswanath V, Nair S S, Subodh G and Muneera C I 2019 *SN Appl. Sci.* **1** 43
- [46] Pramodini S and Poornesh P 2014 *Opt. Laser Technol.* **62** 12
- [47] Singh V and Aghamkar P 2012 *Appl. Opt.* **51** 2288
- [48] Pramodini S, Deepika S, Rao A and Poornesh P 2014 *Opt. Laser Technol.* **62** 58